Research Square

Preprints are preliminary reports that have not undergone peer review.
They should not be considered conclusive, used to inform clinical practice,
or referenced by the media as validated information.

STING Beyond Immunity: Tumour-Intrinsic Roles in Breast Cancer Progression and Metastasis

Vaibhavi Joshi
University of Queensland
Kate Beecher
University of Queensland
Pascal HG Duijf
University of Adelaide
Andrew Stacey
Queensland Health
Sam Druskovich
Queensland Health
Sarah Reed
University of Queensland
Peter T Simpson
University of Queensland
Sunil R Lakhani
University of Queensland
Amy E McCart Reed
amy.reed@uq.edu.au
University of Queensland

Research Article

Keywords: STING, breast cancer, brain metastasis, tumour intrinsic, biomarker

Posted Date: June 5th, 2026

DOI: https://doi.org/10.21203/rs.3.rs-9535798/v1

License: This work is licensed under a Creative Commons Attribution 4.0 International License.
Read Full License

Additional Declarations: No competing interests reported.

Abstract

Purpose

Stimulator of Interferon Genes (STING) is a key inducer of type I interferon signalling that promotes immune cell activation and antitumour immune responses. Reduced STING expression has been reported in multiple tumour types, and STING agonists for their purpose of eliciting an anti-tumour immune response, have emerged as a promising strategy in cancer immunotherapy, including in triple-negative breast cancer. However, the role of STING activation within the tumour cells remains largely unexplored. As STING agonists are increasingly being considered for TNBC clinical trials, defining how tumour-intrinsic STING activation influences breast cancer progression and metastasis is critical for the effective therapeutic exploitation of this pathway.

Methods

We investigated tumour-intrinsic STING expression in breast cancer using phosphorylated STING (pSTING) as a marker of pathway activation. pSTING expression was assessed by immunohistochemistry in two independent cohorts: a breast cancer clinical cohort consisting of 546 BC tumours with > 25 years of clinical follow-up, and a BrM cohort consisting of 81 BrM tumours including 50 matched BC-BrM pairs. To define tumour-intrinsic biological programs associated with STING activation, quantitative proteomic profiling was performed following STING overexpression and knockdown in TNBC cells.

Results

Low or absent pSTING expression in primary tumours was significantly associated with poorer breast cancer–specific survival at both 5 years and 30 years ($P = 0.0009$, $P < 0.001$). While pSTING expression was not associated with survival following brain metastasis surgery, patients with pSTING-high primary tumours exhibited a significantly longer time to brain metastasis development ($P = 0.0112$). Integrative network and pathway analyses revealed coordinated proteomic reprogramming, including upregulation of ribosomal and translational machinery and suppression of metabolic and epithelial–mesenchymal transition–associated programs.

Conclusion

Collectively, our findings demonstrate that tumour-intrinsic STING activation is associated with favourable prognosis, delayed brain metastasis development, and coordinated proteomic reprogramming, highlighting a tumour-intrinsic dimension of STING biology beyond immune activation alone.

1. Introduction

The last two decades have seen a significant increase in work surrounding the role of stimulator of interferon genes (STING) in infectious diseases and cancer. STING, encoded by *TMEM173*, is an endoplasmic reticulum-resident transmembrane protein which plays a central part in the cyclin GMP-AMP synthase (cGAS)-STING pathway, is a key sensor of cytosolic DNA and initiator of innate immune response [1]. While initially studied for its role in host defences against pathogens, the cGAS-STING axis has emerged as a central player in tumour surveillance and anti-tumour immunity [2, 3].

Deficiency of the cGAS-STING pathway within tumour cells is associated with immune evasion [4, 5], underscoring the therapeutic potential of STING activation in various cancers, including breast cancer (BC) [6]. In BC, especially in *BRCA1/2*-mutated, triple-negative breast cancer (TNBC), STING agonists have shown preclinical promise: *in vivo* treatment with the PARP inhibitor olaparib activated the cGAS-STING pathway, enhancing cytotoxic T cell infiltration and anti-tumour immunity in mice [7]. Along with the immune cell stimulation and recruitment, CRISPR-mediated STING knockout in BC cell lines also resulted in complete abolition of olaparib-induced T cell infiltration *in vivo* [7], highlighting the importance of tumour cell- intrinsic STING signaling in therapeutic efficacy.

The consequences of STING activation in cancer cells can range from cell cycle arrest to tumour promotion. Chronic stimulation of cGAS-STING due to micronuclei induced chromosomal instability inactivates interferon signaling and instead promotes the progression of metastasis through downstream non-canonical NFkB signalling [8]. In the context of brain metastasis (BrM), STING activation in astrocytes, facilitated by gap junction proteins such as connexin 43, has been shown to promote pro-inflammatory cytokine release, activating STAT1 and NF-κB pathways in adjacent breast cancer cells and supporting tumour growth, therapy resistance, and brain colonization [9]. STING also exerts non-immunological roles and could also be implicated in promoting tumour growth [10, 11]. In Non-Small Cell Lung Cancer driven by *KRAS/LKB1* mutations (KL NSCLC), LKB1-mediated suppression of STING facilitates immune evasion and aggressive growth {Kitajima, 2019 #50}. Collectively, these contrasting findings reveal the complex, context dependent role of STING in cancer [12].

The cGAS–STING pathway has emerged as a promising target in cancer immunotherapy, with STING agonists currently being evaluated in clinical trials, particularly in combination with immune checkpoint inhibitors for advanced and metastatic tumours including triple-negative breast cancer (TNBC) [13, 14]. These strategies are largely predicated on the ability of STING activation to stimulate anti-tumour immunity through type I interferon signalling and modulation of the tumour microenvironment. However, despite this clinical interest, the tumour-intrinsic roles of STING remain poorly understood. In this study, we examine the tumour cell-intrinsic expression of activated STING in breast cancer progression and metastasis to refine our understanding of STING's context-dependent role in tumour cells and evaluate its therapeutic potential in both primary and metastatic breast cancer.

2. Results

2.1 Clinicopathological Analysis of pSTING in Breast Cancer

To contextualise STING pathway expression in breast cancer, *TMEM173* mRNA levels were assessed in The Cancer Genome Atlas (TCGA) dataset. Compared to normal breast tissue, *TMEM173* mRNA was significantly reduced in breast cancer overall. However, expression levels were comparable across PAM50 molecular subtypes and tumour stage (**Figure S1**).

To understand the STING pathway at the protein level, immunohistochemistry was performed for total STING and phosphorylated STING (pSTING; 'activated') in primary breast cancers from the Queensland Follow Up (QFU) cohort [15], which comprises 564 breast cancer patients. While no significant associations were observed for total STING expression (**Figure S2**), analysis of pSTING revealed notable clinicopathological correlations. In the QFU cohort, 92% of the cases showed tumour cell specific expression of pSTING and were stratified as moderate or high (Fig. 1).

A statistically significant relationship between pSTING positivity and histological subtype was not identified **(**Fig. 2a**)**. However, negative and moderate pSTING expression was significantly associated with poorer breast cancer specific survival (BCSS) across all tumours at 5 years (Fig. 2b; P = 0.0193, Log-rank). In the longer term, negative pSTING expression showed a pronounced association with poorer survival beyond 10 years, persisting through to 30 years (Fig. 2c; P = < 0.0001, Log-rank). pSTING distribution was similar across ER+, HER2+, and TNBC subtypes, with moderate expression being dominant across all three (Fig. 2d). Lack of pSTING expression across ER+ (Fig. 2e, P = 0.023), and HER2+ (Fig. 2f, P = 0.0485) BC cases associated with significant poorer BCSS at 30 years, and although not significant, a similar trend was observed for TNBC cases (Fig. 2g, P = 0.2020).

pSTING expression was unevenly distributed across tumour grade (Fig. 2h; P = 0.0035, Chi-square). High pSTING expression significantly associated with improved BCSS across grade 1 (Fig. 2i; P = 0.0118, Log-rank), grade 2 (Fig. 2j; P = 0.026, Log-rank) and grade 3 at the 30-year time point (Fig. 2k; P = 0.026, Log-rank). We next investigated the association of pSTING expression with immune features within our cohort. Immune infiltration was assessed in two ways: (i) lymphocytic infiltrate (LI), reflecting the overall extent of lymphocyte infiltration across the tumour and (ii) tumour-infiltrating lymphocytes (TILs) scored specifically within the tumour stroma, in accordance with the International TILs Working Group [16]. Higher overall LI was associated with lack of pSTING expression **(Figure S3a)**. This relationship was also significant in TNBC, consistent with the finding that negative pSTING is linked to worse prognosis **(Figure S3a)**. No significant association between pSTING expression and TILs was observed (**Figure S3b**).

Table 1 contains the clinicopathological characteristics of breast cancer tumours stratified by pSTING expression. Tumour size and grade were inversely associated with pSTING expression, with no significant associations with age, lymph node status and prognostic subtypes observed.

Table 1
Clinicopathological characteristics of breast cancer tumours stratified by pSTING expression.

	Negative n (%)	Moderate n (%)	High n (%)	P value	Statistical test
Age of Diagnosis (years)					
> 40	36 (87.80%)	352 (90.49%)	114 (87.69%)	0.6122	Chi-square
< 40	5 (12.20%)	37 (9.51%)	16 (12.31%)		
Total	41 (8.04%)	339 (66.47%)	130 (25.49%)	-	-
Tumour Size (cm)					
< 2	20 (60.61%)	104 (40.94%)	36 (61.02%)	**0.0164**	Chi-square
2–5	12 (36.36%)	120 (47.24%)	20 (33.90%)		
> 5	1 (3.03%)	30 (11.81%)	3 (5.084%)		
Tumour Grade					
1	6 (9.52%)	34 (53.97%)	23 (36.51%)	**0.0035**	Chi-square
2	26 (9.96%)	182 (69.73%)	53 (20.31%)		
3	8 (3.54%)	165 (73.01%)	53 (23.45%)		
Lymph Node Status					
Negative	7 (30.43%)	99 (52.66%)	23 (62.16%)	0.0552^	Fisher's exact test
Positive	16 (69.57%)	89 (47.34%)	14 (37.84%)		
Prognostic Subtypes					
ER+	7 (11.86%)	44 (74.58%)	8 (13.56%)	0.2030	Chi-square
HER2+	19 (7.14%)	170 (67.29%)	68 (25.56%)		
TNBC	4 (7.018%)	43 (75.44%)	10 (17.54%)		
Histological Subtypes					
IC-NST	21 (5.9%)	243 (68.5%)	91 (25.6%)	0.3428	Chi-square
Lobular	9 (13%)	51 (73.9%)	9 (13%)		

	Negative n (%)	Moderate n (%)	High n (%)	P value	Statistical test
Age of Diagnosis (years)					
Mixed ductal/lobular	4 (9.9%)	30 (68%)	10 (22.7%)		
Mixed other	2 (5.3%)	28 (73.7%)	8 (21%)		
Other special type	3 (6.8%)	30 (68%)	11 (25%)		

2.2 Clinicopathological Analysis of pSTING in Breast to Brain Metastases

Given that the low expression of pSTING was associated with a poor BCSS, we investigated whether pSTING expression impact outcomes in metastatic breast cancer patients. To investigate this pSTING expression was examined in a series of brain metastatic breast cancers from the Queensland Breast to Brain Metastasis (QBBM) cohort were studied. In total, 60 primary breast cancers and 79 brain metastases were assessed, including 50 cases of matched pairs of primary and brain metastases.

pSTING expression was categorised as low (negative and 1+, Fig. 3a**)** or high (2 + and 3+, Fig. 3b, Table 2). The proportions of pSTING low and high expression were similar across both BC and BrM tumours **(**Fig. 3c**)** and when stratified by prognostic subtype **(**Fig. 3d**).** Breast cancer specific survival and brain metastasis specific survival showed no prognostic associations with pSTING either for all cases combined **(Figure S4a-c)**, or across BC prognostic subtypes **(Figure S4d-l)**. pSTING status was also compared across matched BC-BrM cases to record the expression change in BrMs from the primary tumour (**Figure S5a-c**).

Time to neurosurgery post breast cancer diagnosis was compared in pSTING high and pSTING low patients as a surrogate for time taken to develop symptomatic brain metastasis. In univariate analysis, BC patients with low pSTING expression had a significantly shorter time to neurosurgery following primary BC diagnosis, as compared with those with high pSTING expression (Fig. 3e; P = 0.0112 Welch's t-test). Broadly, TNBC had a shorter time to neurosurgery regardless of pSTING status; HER2 positive cases from this cohort would have been eligible for anti-HER2 therapy.

To evaluate whether the protective association of pSTING expression was independent of prognostic breast cancer subtype, we performed a general linear model analysis with time to neurosurgery as the dependent variable and pSTING expression and prognostic subtype (ER+, HER2+, TNBC) as independent variables (**Table S1**). The overall model did not reach statistical significance ($F(5,53) = 2.29$, $P = 0.059$). Neither pSTING expression ($F(1,53) = 3.51$, $P = 0.067$) nor breast cancer prognostic subtype ($F(2,53) = 2.13$, $P = 0.128$) showed an independent association with time to neurosurgery.

Table 2
Clinicopathological characteristics of BC-BrM stratified by pSTING expression.

		Low	High	P value	Statistical test
Brain Metastatic Primary Breast Cancer					
	Total	20 (33%)	40 (66%)	-	-
HR Status	ER+	4 (24%)	13 (76%)	0.4884	Chi-square
	HER2+	5 (31%)	11 (69%)		
	TNBC	11 (41%)	16 (59%)		
Grade	1	0 (0%)	1 (100%)	0.2546	Chi-square
	2	2 (14%)	12 (86%)		
	3	15 (36%)	27 (64%)		
	Total	17 (30%)	40 (70%)		
Time to neurosurgery	Range (Years)	4.6297	17.18	**0.0112**	Welch's t test
Brain metastases					
	Total	39 (49%)	40 (51%)	0.0828	Fisher's exact test*
*Compared to total primary breast cancers					

2.3 Proteomic Analysis of Differentially Expressed Proteins in STING Modulated Cell Lines

The IHC evaluation points to efficacy for pSTING agonists in a subset of BC, however the molecular consequences of tumour activation of pSTING are not clear. Thus, we sought to investigate the molecular mechanisms that underpin these observations. As phosphorylation represents a dynamic activation state, we focused subsequent analyses on total STING expression to study tumour-intrinsic STING-associated pathways. Although STING agonists are currently being tested in clinical trials, particularly in combination with PD-1 inhibitors for metastatic TNBC [13], patient selection is not based on tumoural STING expression. These studies largely assume that STING activation enhances anti-tumour immunity; however, the cellular context in which this occurs within tumour cells remains poorly defined. To explore this tumour-intrinsic function, we performed proteomic analyses of differentially expressed proteins in STING-modulated breast cancer cell lines to delineate the downstream pathways and biological processes associated with STING expression.

Given that the therapeutic relevance of STING has been primarily studied in TNBC [17–19], we selected the MDA-MB-231 (TNBC) cell line to investigate STING-associated proteins and signalling pathways using mass spectrometry. Cells were transduced with lentiviral constructs to generate STING-

overexpressing (STING-high) and STING-silenced (STING-low) models, alongside an empty vector control (Fig. 4a). Western blotting confirmed successful modulation of STING expression (Fig. 4a). An unbiased mass spectrometry-based global proteome approach was performed. Information-dependent acquisition (IDA) and SWATH profiles from each group were analysed using PeakView software, for identifying distinct peptides and proteins (Fig. 4b). Differentially expressed proteins (DEPs) were identified by normalising STING-high and low cells to the parental cells as a control group and Log2fold change values were used to quantify the differential protein expression. Additionally, DEPs were also identified for STING-High compared to STING-Low group. DEPs were identified using a two-sample t-test (cut-off $P < 0.05$) and visualised as volcano plots for the three comparisons (Fig. 4a-e). 110 significant DEPs were identified in STING-high (Fig. 4c, 45 upregulated and 65 downregulated proteins) and 99 significant DEPs in STING-low (Fig. 4d, 57 upregulated and 42 downregulated proteins) groups, when compared to control. For STING high vs STING-low, a total of 170 DEPs were identified (Fig. 4e, 75 upregulated and 95 downregulated).

2.4 Functional Enrichment Analysis of STING Associated Proteins in Breast Cancer Cell Lines

Protein–protein interaction (PPI) network analysis focussed on DEPs identified between STING-high and STING-low MDA-MB-231 cells was performed using the STRING database and visualised in *Cytoscape* (Fig. 5a). Network topology analysis using *cytoHubba* identified the top 10 hub proteins based on maximal clique centrality (MCC). All hub proteins were upregulated in STING-high cells and consisted exclusively of ribosomal proteins belonging to the large (60S) ribosomal subunit, indicating a strong association between STING expression and the translational machinery.

Gene Ontology (GO) over-representation analysis (*g:Profiler*; **Table S2.1, S2.2**) found upregulated proteins with a strong enrichment for ribosome- and translation-associated functions (Fig. 5b), including molecular functions (MF) related to RNA binding and aminoacyl-tRNA ligase activity, biological processes (BP) involved in cytoplasmic translation and ribosome biogenesis, and cellular components (CC) associated with the cytosolic ribosome and endoplasmic reticulum. Cadherin binding was also enriched. In contrast, downregulated proteins were enriched for metabolic and RNA-processing functions (Fig. 5c), including catabolic processes, the tricarboxylic acid (TCA) cycle, RNA binding, and spliceosome-associated activities.

To interrogate pathway-level alterations, over-representation analysis was performed using *Enrichr* with KEGG and *MSigDB* Hallmark pathway databases. Consistent with PPI network and GO enrichment analyses, KEGG pathway enrichment highlighted ribosome-associated pathways among upregulated proteins, while downregulated proteins were enriched for metabolic pathways (Fig. 6a). MSigDB Hallmark analysis identified enrichment of MYC targets and interferon-α response pathways among upregulated proteins, whereas epithelial–mesenchymal transition (EMT) and adipogenesis pathways were enriched among downregulated proteins (Fig. 6b). The MYC Targets V1 pathway was significantly enriched among both upregulated and downregulated proteins in STING- high cells. However, enrichment

was driven by different protein subsets in each case (**Table S3**), underscoring the complex and dynamic nature of MYC-associated signaling. In agreement with these findings, rank-based gene set enrichment analysis (GSEA) of a pre-ranked (fold-change) list of all quantified proteins revealed significant negative enrichment of EMT and adipogenesis programs in STING-high relative to STING-low cells (Fig. 6c,d). Additional enrichment analyses comparing STING-high and STING-low cells to control cells are shown in **Figure S6a–g**.

Collectively, these analyses demonstrate that differential STING expression is associated with coordinated remodelling of translational, metabolic, and mesenchymal-associated protein networks in breast cancer cells.

2.5 Transcriptomic analysis in the AURORA dataset

Finally, to determine whether STING-associated tumour-intrinsic proteomic programs were reflected at the transcriptomic level in metastatic disease, we analysed the AURORA cohort [20]. *TMEM173* mRNA expression was first examined in matched primary breast cancer–brain metastasis pairs (n = 7), revealing a significant reduction in *TMEM173* expression in brain metastases compared with their matched primary tumours (Fig. 7a**).** Given that proteomic analyses identified high STING expression to be associated with negative enrichment of epithelial–mesenchymal transition (EMT)–related pathways, *CDH1* expression was next evaluated in primary breast cancer cases stratified by *TMEM173* expression. *CDH1* expression demonstrated a near-significant association with STING-high breast cancers (Fig. 7b; STING-high = 11, STING-low = 12). To understand whether proteomics-derived pathway alterations were reflected at the gene expression level, composite RNA expression z-scores were calculated for genes encoding proteins identified in the proteomics-derived EMT and Estrogen Response Late signatures. Neither the EMT-associated gene signature (Fig. 7c) nor the Estrogen Response Late gene signature (Fig. 7d) showed a significant association with *TMEM173* expression in primary breast cancer cases, suggesting that these pathway alterations may be regulated at the post-transcriptional or post-translational level.

3. Discussion

In this study, we investigated tumour-intrinsic STING activation in breast cancer and brain metastasis, with the aim of defining its prognostic relevance and the biological programs associated with activated STING signalling within tumour cells. While STING has been extensively studied in the context of immune sensing and tumour–microenvironment interactions [1], its role within tumour epithelial cells remains less well characterised. To address this, we focused on phosphorylated STING (pSTING) as a marker of pathway activation, recognising that total STING expression alone does not necessarily reflect functional engagement of the cGAS–STING pathway.

We demonstrate that pSTING expression in primary breast tumours is associated with improved breast cancer–specific survival, supporting a tumour-suppressive role for STING activation in early disease.

Importantly, our study extends previous observations by assessing activated STING directly, rather than relying on indirect measures such as total STING expression or inferred subcellular localisation [21–23]. In contrast to earlier studies [21–23] that examined tumour-intrinsic STING using perinuclear localisation or downstream signalling components, our phospho-specific approach provides a more direct readout of STING pathway activation. The large size of our cohort further enabled robust stratification across tumour grades and subtypes, strengthening the observed associations.

We explored the relationship between tumour-intrinsic STING activation and metastatic outcomes, with a particular focus on brain metastases. pSTING expression within brain metastases was not associated with post-metastatic outcomes, understandably given the limited clinical follow up period in these poor prognostic cases. However, high pSTING expression in primary tumours was associated with a significantly longer time to brain metastasis development. Thus tumour-intrinsic STING activation may have an influence in delaying metastatic progression.

To gain mechanistic insight, we performed quantitative proteomic profiling following direct modulation of STING expression in triple negative breast cancer cells. This experimental approach allowed us to interrogate tumour-intrinsic STING-associated programs independently of microenvironmental contributions, an aspect not addressed in prior transcriptomic or correlative studies. Protein–protein interaction network analysis identified ribosomal proteins of the 60S subunit as dominant hubs in STING-high cells, and pathway enrichment analyses revealed strong over-representation of ribosome-associated and translational processes. These findings suggest that STING activation is linked to coordinated regulation of protein synthesis machinery within tumour cells.

The enrichment of translational machinery in STING-high cells agrees with the emerging evidence that components of the cGAS–STING pathway may be involved in processes linked with stress beyond DNA sensing, including disruption of ribosome-associated protein production pathways [24, 25]. Enrichment of aminoacyl-tRNA ligase activity further supports a link between STING activation and translational regulation, although whether this reflects enhanced translational capacity or a compensatory stress response remains to be determined. In parallel, Hallmark pathway analysis revealed suppression of estrogen response late signalling in STING-high cells, a program associated with resistance and poorer outcomes in breast cancer [26, 27]. The downregulation of this pathway in STING-high cells suggests that tumour-intrinsic STING activation may modulate hormone-responsive transcriptional states, potentially contributing to a less aggressive tumour phenotype.

In addition to translational reprogramming, STING-high cells exhibited features consistent with suppression of mesenchymal and metastatic phenotypes. Enrichment of cadherin binding and focal adhesion-related components, together with a reduction in epithelial–mesenchymal transition gene sets, indicates preservation of epithelial characteristics in STING-high cells. These findings provide a potential biological link to the delayed development of brain metastases observed in patients with pSTING-high primary tumours.

Metabolic pathways also emerged as a distinguishing feature between STING-high and STING-low states. Proteins downregulated in STING-high cells were enriched for metabolic and RNA-processing functions, including tricarboxylic acid cycle–related pathways and adipogenesis-associated programs. As metabolic plasticity is increasingly recognised as a driver of tumour aggressiveness and metastatic progression [28], the suppression of these pathways in STING-high cells is consistent with a more restrained tumour phenotype and may contribute to the observed tumour-suppressive associations.

To extend our proteomic findings beyond experimental models, we interrogated external patient datasets to assess tumour-intrinsic STING-associated changes at the transcriptomic level. Notably, *TMEM173* expression was significantly reduced in matched primary breast cancer–brain metastasis pairs, consistent with attenuation of STING signalling during metastatic progression and supporting a model in which STING-active tumour cells are selected against during dissemination.

Several limitations of this study should be acknowledged. The QFU cohort is an archival cohort with patients diagnosed before 1995 and hence did not receive the current contemporary treatments. Proteomic analyses were performed in a single breast cancer cell line, and validation across additional models will be necessary to strengthen these findings. The current analyses also provide a static snapshot of STING-associated proteomic states and do not capture dynamic changes following acute pathway activation or suppression. Furthermore, while this study focused on tumour-intrinsic STING signalling, integration of immune context, including assessment of tumour-associated immune infiltrates in relation to pSTING expression, may provide additional insight. Finally, proteomic profiling of brain metastasis tumour cells represents an important future direction to determine whether STING-associated programs differ between primary and metastatic sites.

In summary, our study demonstrates that activated tumour-intrinsic STING is associated with favourable prognosis in primary breast cancer and delayed development of brain metastases. Through direct modulation of STING expression and quantitative proteomic profiling, we identify changes in translational, metabolic, hormonal, and EMT-associated programs that extend beyond immune activation alone. These findings highlight a previously underappreciated tumour-intrinsic dimension of STING biology and suggest that STING activation may influence breast cancer progression by constraining tumour cell states associated with aggressiveness and metastasis. Further investigation of these mechanisms may inform risk stratification and therapeutic strategies targeting STING signalling in breast cancer.

4. Material and Methods

4.1 Clinical Cohorts

The ethical approval was received from the Royal Brisbane Women’s Hospital (RBWH) (2005/022) and The University of Queensland (2005000785) for the use of clinical data and samples from patients.

Two clinical cohorts were utilised in this study: (1) the Queensland Follow-Up (QFU) cohort, consisting of 564 formalin-fixed paraffin-embedded (FFPE) breast tumour samples from patients that underwent breast tumour resection at the Royal Brisbane Women's Hospital between 1987 and 1994, along with their long-term clinical follow-up information (median 11.85 years; range: 0.03 to 41 years) [31]. (2) Queensland Breast cancer-Brain Metastasis (QBBM) cohort comprised of brain-metastatic breast cancer patients (n = 60) and brain metastasis (BrM) samples (n = 81), including 50 matched breast cancer-BrM pairs, treated between the years 2000 and 2018 [56]. All HER2 + patients in the QBBM cohort were diagnosed after 2000 and therefore would have been eligible to receive Herceptin.

Tumour regions were incorporated as tissue microarrays (TMAs) with core diameters of 0.6 mm for the QFU cohort and 1 mm for the QBBM cohort and subsequently used for immunohistochemical (IHC) analyses. Clinicopathological data, including diagnostic details, pathology reports, and outcome information, were obtained from Pathology Queensland, Queensland Health, and the Queensland Cancer Registry.

Survival outcomes were evaluated as breast cancer–specific survival (BCSS), defined as the interval from primary breast cancer diagnosis to the date of last follow-up, and brain metastasis–specific survival (BrMSS), defined as the time from brain metastasis resection to the most recent follow-up.

4.2 Immunohistochemistry

FFPE tissue sections (4 µm) were subjected to heat-induced epitope retrieval using a decloaking chamber (NexGen, Biocare Medical, Concord, CA, USA) in 0.01 M sodium citrate buffer (pH 6.0) at 110°C for 20 min. To block endogenous peroxidase activity, the sections were incubated in 3% hydrogen peroxide (H_2O_2) for 10 min. Immunohistochemical staining was performed using reagents from the MACH1 Universal HRP Detection Kit (Biocare Medical, LLC, Concord, CA, USA; #M1U539 L10). To minimise non-specific binding, sections were incubated with MACH1 Sniper blocking reagent for 30 min. Primary antibodies targeting STING (1:250; Invitrogen, clone OT14H1; #MA5-26030) and phospho-STING (1:100); Thermo Fisher Scientific; clone Ser366; #PA5-105674) were prepared in Biocare Da Vinci Green Diluent (Biocare Medical; #PD900) and applied overnight at room temperature. Sections were subsequently incubated with the MACH1 secondary antibody conjugated to a horseradish peroxidase polymer for 30 min at room temperature. Signal detection was achieved using the MACH1 diaminobenzidine substrate, followed by counterstaining with hematoxylin.

4.3 Scoring and analysis

Immunohistochemical scoring was performed in collaboration with experienced pathologists. STING expression in QFU and QBBM cases was assessed by Dr Andrew Stacey, while phosphorylated STING (pSTING) in the same cases was evaluated by Dr Sam Druskovich. Positivity for total STING and phospho-STING was defined as > 1% of tumour cells exhibiting unequivocal staining, with < 1% classified as negative.

For the QFU cohort, cases were further stratified into negative, moderate (combined 1 + and 2+), or high (3+) expression groups. Due to the smaller sample size of the QBBM cohort, cases were categorised as low (negative and 1+) or high (2 + and 3+) expression for downstream analyses. Lymphocytic infiltration and tumour infiltrating lymphocytes were scored as described previously [29].

4.4 Cell Culture and Lentiviral Transduction

MDA-MB-231 human breast cancer cells were obtained from the American Type Culture Collection (ATCC) and cultured in Dulbecco's Modified Eagle Medium (DMEM, Gibco/#1195065) supplemented with 10% fetal bovine serum (Gibco, Invitrogen, Cat# 10099141) and 1× antibiotic–antimycotic (Gibco, Invitrogen, Cat# 11360). Cells were maintained at 37°C in a humidified atmosphere containing 5% CO_2 and routinely passaged using TrypLE (Life Technologies, Cat# 12605010)) prior to reaching full confluency. Cell numbers were determined using an Invitrogen Countess™ (C10227) automated cell counter.

Lentiviral constructs encoding empty vector control (VB010000-9298rtf), overexpression (VB900083-594mxp), or shRNA (VB900090-7227ftv) STING were purchased from VectorBuilder (USA). Cells were transduced in antibiotic-free medium at approximately 50% confluency using a multiplicity of infection (MOI) of 5 in the presence of polybrene (8 µg/mL). After 16 h, viral supernatant was replaced with complete medium, and cells were cultured for an additional 72 h. Stable transduction was monitored by enhanced green fluorescent protein (EGFP) expression using the IncuCyte S3 live-cell analysis system (Essen Bioscience), and transduced populations were enriched by puromycin selection.

4.5 Western blot

Protein concentrations were determined using the Pierce BCA Protein Assay Kit (Thermo Scientific, Rockford, IL, USA; #23225). Equal amounts of protein (20 µg) were separated on 4–12% Bis–Tris SDS–PAGE gels (Bolt, Invitrogen, Thermo Fisher Scientific) and transferred onto polyvinylidene fluoride (PVDF) membranes (Millipore, MA, USA; #IPVH00010). Membranes were blocked for 1 h in 5% bovine serum albumin (BSA) prepared in Tris-buffered saline containing 0.1% Tween-20 (TBST; Sigma Life Science, MO, USA; #P2287). Blots were incubated overnight at 4°C with primary antibodies against STING (1:1000; Cell Signaling Technology, clone D2P2F; #13647) or vinculin (1:1000; Sigma-Aldrich; #V9131), followed by incubation with horseradish peroxidase–conjugated secondary antibodies (anti-mouse or anti-rabbit) for 1 h at room temperature. Protein signals were detected using SuperSignal™ West Pico PLUS chemiluminescent substrate (Thermo Fisher Scientific).

4.6 Mass Spectrometry and Bioinformatic Analysis

Protein samples were processed for mass spectrometry using filter-aided sample preparation (FASP). Briefly, equal amounts of protein lysate were reduced, alkylated, and digested with trypsin using centrifugal filter units (10 kDa cutoff), followed by peptide desalting using C18 ZipTips (Millipore). Desalted peptides were dried and resuspended prior to analysis. Liquid chromatography–tandem mass

spectrometry (LC–MS/MS) was performed at the Frazer Institute Mass Spectrometry Facility using a SCIEX ZenoTOF 7600 system.

Protein identification and quantification were performed using a data-independent acquisition (SWATH) workflow. Proteins passing a 1% false discovery rate (FDR) threshold were retained for downstream analysis. Differentially expressed proteins were identified based on fold change and statistical significance, with expression changes reported as $\log_2$ fold change relative to control conditions.

Protein–protein interaction networks were constructed using the STRING database [30] via Cytoscape (v3.10.1) [31]. Network topology analysis was performed using the cytoHubba plugin to identify the top 10 hub proteins based on maximal clique centrality (MCC). Functional enrichment of differentially expressed proteins was assessed using over-representation analysis (ORA) for Gene Ontology (GO) terms with g:Profiler [32]. Additional ORA was performed for KEGG pathways and MSigDB gene sets using Enrichr [33]. Gene set enrichment analysis (GSEA) was performed in R using the fgsea package, with gene sets obtained from MSigDB via the msigdbr package. Human gene annotations were mapped using org.Hs.eg.db and ranked protein lists based on $\log_2$ fold change were used as input for enrichment analysis.

4.7 Estimation of *TMEM173* mRNA expression in breast cancer

Batch effects-normalized mRNA levels ($log2\ (normalized\ counts$+1) values) using Illumina HiSeq RNASeqV2 were obtained from the pan-cancer dataset of The Cancer Genome Atlas (TCGA) [58]. Spearman R and p values were determined in R (version 4.3.1; The R Project for Statistical Computing) and boxplots were created using the tidyverse package.

4.8 Transcriptomic analysis of the AURORA dataset

Publicly available RNA-sequencing data from the AURORA-US metastatic breast cancer dataset (GSE193103) [20, 34] were analysed. Transcript abundance values (transcripts per million; TPM) were $\log_2$-transformed prior to analysis. A total of 23 primary breast cancer cases were included, along with 7 matched primary and brain metastasis samples. For patients with multiple lesions of the same tissue type, gene expression values were averaged to obtain patient-level measurements. Genes identified from MSigDB proteomic analyses relating to epithelial–mesenchymal transition (EMT) and estrogen response late pathways were evaluated in the AURORA dataset. For each gene signature, expression values were z-score normalised per gene across samples, and a composite signature score was calculated as the mean z-score across all genes within the signature. Cases were stratified as STING-high or STING-low using the median *TMEM173* expression across primary tumours for each analysis. Differences in signature scores between STING-high and STING-low groups were assessed using the Wilcoxon rank-sum test. All analyses were conducted at the patient level, and p-values < 0.05 were considered statistically significant.

4.9 Statistical Analysis

Statistical analyses were performed using GraphPad Prism (version 9.0) and IBM SPSS statistics (version 30.0.0). Univariate comparisons were conducted using Welch's t-test. To evaluate the association between STING expression and time to neurosurgery while adjusting for breast cancer subtype, a general linear model (GLM) was applied with time to neurosurgery treated as a continuous dependent variable. STING expression (low vs high) and breast cancer subtype (ER+, HER2+, and TNBC) were included as fixed factors, and an interaction term was tested. As all patients underwent neurosurgical intervention, survival-based models were not applied. Statistical significance was defined as $P < 0.05$.

Declarations

Acknowledgements

We thank all the patients who donated tissue for research purposes. We acknowledge the support of Metro North Hospital and Health Services for the collection of the clinical subject data and clinical subject materials. We would also like to thank FI Mass spectrometry facility (MSF) especially Aven Lee for their support and guidance.

Patient consent statement

All patients provided written, informed consent to the use of their tissues for research or were approved under Public Health Access agreement.

Ethics Declaration

This study was conducted in accordance with the Declaration of Helsinki. Ethics approval was granted by The Royal Brisbane Women Hospital and University of Queensland Human Research Ethics Committee (approval number 2005000785/HREC/2005/022). Written informed consent was obtained from all participants, or a waiver approved by the Public Health Act.

Funding

This research was funded by the National Health and Medical Research Council (APP1113867).

Author Contributions

VJ, and AMR designed the project. VJ, and KB performed the experiments and analysed/interpreted the results. VJ, AS, and SD analysed/interpreted the clinical data. VJ, KB, and AMR wrote the manuscript. PHD conducted the transcriptomic analysis of the TCGA dataset. VJ and SR performed and analysed proteomics experiments. AMR, PS, and SRL provided supervision, and conceptualization. AMR and SRL acquired funding. All authors reviewed and approved the manuscript.

Competing Interests

The authors declare no competing financial interests.

Data Availability Statement

The datasets generated during and/or analysed during the current study are available from the corresponding author on reasonable request.

References

1. H. Ishikawa, G.N. Barber, STING is an endoplasmic reticulum adaptor that facilitates innate immune signalling. Nature. **455**(7213), 674–678 (2008)
2. H. Ishikawa, Z. Ma, G.N. Barber, STING regulates intracellular DNA-mediated, type I interferon-dependent innate immunity. Nature. **461**(7265), 788–792 (2009)
3. L. Sun et al., Cyclic GMP-AMP synthase is a cytosolic DNA sensor that activates the type I interferon pathway. Science. **339**(6121), 786–791 (2013)
4. T. Xia et al., Deregulation of STING Signaling in Colorectal Carcinoma Constrains DNA Damage Responses and Correlates With Tumorigenesis. Cell. Rep. **14**(2), 282–297 (2016)
5. T. Xia, H. Konno, G.N. Barber, Recurrent Loss of STING Signaling in Melanoma Correlates with Susceptibility to Viral Oncolysis. Cancer Res. **76**(22), 6747–6759 (2016)
6. E.E. Parkes et al., Activation of a cGAS-STING-mediated immune response predicts response to neoadjuvant chemotherapy in early breast cancer. Br. J. Cancer. **126**(2), 247–258 (2022)
7. C. Pantelidou et al., PARP Inhibitor Efficacy Depends on CD8(+) T-cell Recruitment via Intratumoral STING Pathway Activation in BRCA-Deficient Models of Triple-Negative Breast Cancer. Cancer Discov. **9**(6), 722–737 (2019)
8. S.F. Bakhoum et al., Chromosomal instability drives metastasis through a cytosolic DNA response. Nature. **553**(7689), 467–472 (2018)
9. Q. Chen et al., Carcinoma–astrocyte gap junctions promote brain metastasis by cGAMP transfer. Nature. **533**(7604), 493–498 (2016)
10. J. Ahn et al., Inflammation-driven carcinogenesis is mediated through STING. Nat. Commun. **5**(1), 5166 (2014)
11. S.F. Bakhoum et al., Chromosomal instability drives metastasis through a cytosolic DNA response. Nature. **553**(7689), 467–472 (2018)
12. K.R.B. Lanng, E.L. Lauridsen, M.R. Jakobsen, The balance of STING signaling orchestrates immunity in cancer. Nat. Immunol. **25**(7), 1144–1157 (2024)
13. K.J. Harrington et al., Phase I and II Clinical Studies of the STING Agonist Ulevostinag with and without Pembrolizumab in Participants with Advanced or Metastatic Solid Tumors or Lymphomas. Clin. Cancer Res. **31**(16), 3400–3411 (2025)
14. F. Meric-Bernstam et al., Phase Ib study of MIW815 (ADU-S100) in combination with spartalizumab (PDR001) in patients (pts) with advanced/metastatic solid tumors or lymphomas. J. Clin. Oncol.

37(15suppl), 2507–2507 (2019)

15. J.R. Kutasovic et al., Breast cancer metastasis to gynaecological organs: a clinico-pathological and molecular profiling study. J. Pathology: Clin. Res. **5**(1), 25–39 (2019)
16. S. Hendry et al., *Assessing tumor-infiltrating lymphocytes in solid tumors: a practical review for pathologists and proposal for a standardized method from the international immunooncology biomarkers working group: part 1: assessing the host immune response, TILs in invasive breast carcinoma and ductal carcinoma in situ, metastatic tumor deposits and areas for further research.* Advances in anatomic pathology, 2017. 24(5): pp. 235–251
17. D. Chandra et al., STING Ligand c-di-GMP Improves Cancer Vaccination against Metastatic Breast Cancer. Cancer Immunol. Res. **2**(9), 901–910 (2014)
18. N. Cheng et al., A nanoparticle-incorporated STING activator enhances antitumor immunity in PD-L1–insensitive models of triple-negative breast cancer. JCI insight, 2018. **3**(22)
19. C. Pantelidou et al., STING agonism enhances anti-tumor immune responses and therapeutic efficacy of PARP inhibition in BRCA-associated breast cancer. NPJ Breast Cancer. **8**(1), 102 (2022)
20. S. Garcia-Recio et al., Multiomics in primary and metastatic breast tumors from the AURORA US network finds microenvironment and epigenetic drivers of metastasis. Nat. Cancer. **4**(1), 128–147 (2023)
21. M. Chen et al., cGAS-STING pathway expression correlates with genomic instability and immune cell infiltration in breast cancer. npj Breast Cancer. **10**(1), 1 (2024)
22. T. Maeda et al., Prognostic Impact of Stimulator of Interferon Genes Expression in Triple Negative Breast Cancer. Cancer Med. **14**(4), e70666 (2025)
23. E.E. Parkes et al., The clinical and molecular significance associated with STING signaling in breast cancer. npj Breast Cancer. **7**(1), 81 (2021)
24. L. Wan et al., Translation stress and collided ribosomes are co-activators of cGAS. Mol. Cell. **81**(13), 2808–2822e10 (2021)
25. J.K. Seok et al., Beyond DNA sensing: expanding the role of cGAS/STING in immunity and diseases. Arch. Pharm. Res. **46**(6), 500–534 (2023)
26. A. Liberzon et al., The Molecular Signatures Database Hallmark Gene Set Collection. Cell. Syst. **1**(6), 417–425 (2015)
27. Z. Li et al., *EstroGene database reveals diverse temporal, context-dependent and directional estrogen receptor regulomes in breast cancer.* bioRxiv, 2023: p. 2023.01.30.526388
28. N.M. Anderson et al., The emerging role and targetability of the TCA cycle in cancer metabolism. Protein Cell. **9**(2), 216–237 (2018)
29. E. Kalaw et al., Metaplastic breast cancers frequently express immune checkpoint markers FOXP3 and PD-L1. Br. J. Cancer. **123**(11), 1665–1672 (2020)
30. D. Szklarczyk et al., The STRING database in 2023: protein-protein association networks and functional enrichment analyses for any sequenced genome of interest. Nucleic Acids Res. **51**(D1),

D638–d646 (2023)

31. P. Shannon et al., Cytoscape: a software environment for integrated models of biomolecular interaction networks. Genome Res. **13**(11), 2498–2504 (2003)
32. J. Reimand et al., g:Profiler–a web-based toolset for functional profiling of gene lists from large-scale experiments. Nucleic Acids Res., 2007. 35(Web Server issue): pp. W193–200
33. E.Y. Chen et al., Enrichr: interactive and collaborative HTML5 gene list enrichment analysis tool. BMC Bioinform. **14**, 128 (2013)
34. S. Garcia-Recio et al., Understanding metastasis mixed-treatment responses through genomic analyses. NPJ Breast Cancer. **11**(1), 9 (2025)

Figures

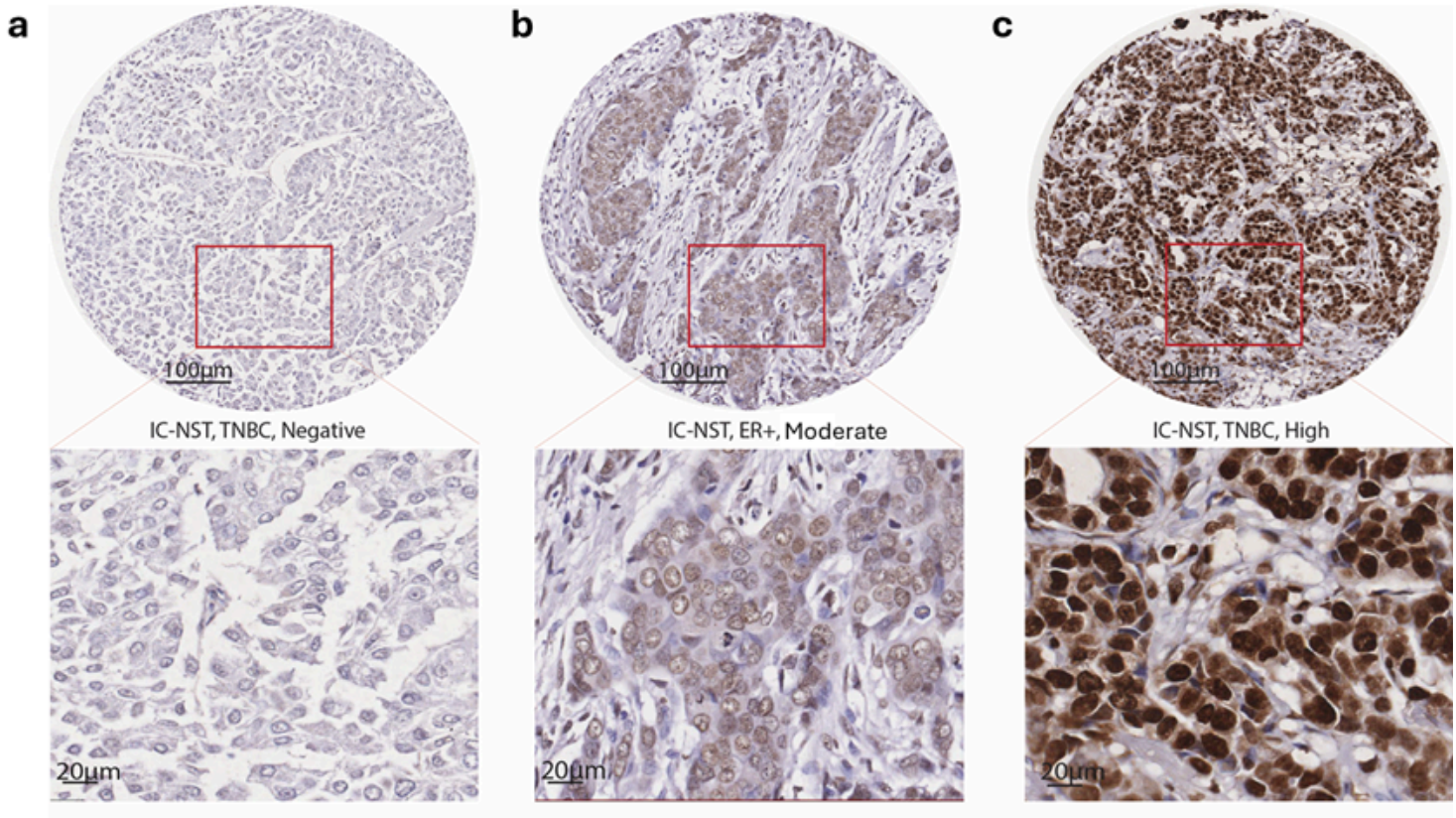


Figure 1

IHC analysis of pSTING expression in breast tumours in the QFU cohort. Representative immunohistochemistry images of breast tumour cores scored as **(a)** negative, **(b)** moderate, and **(c)** high for pSTING.

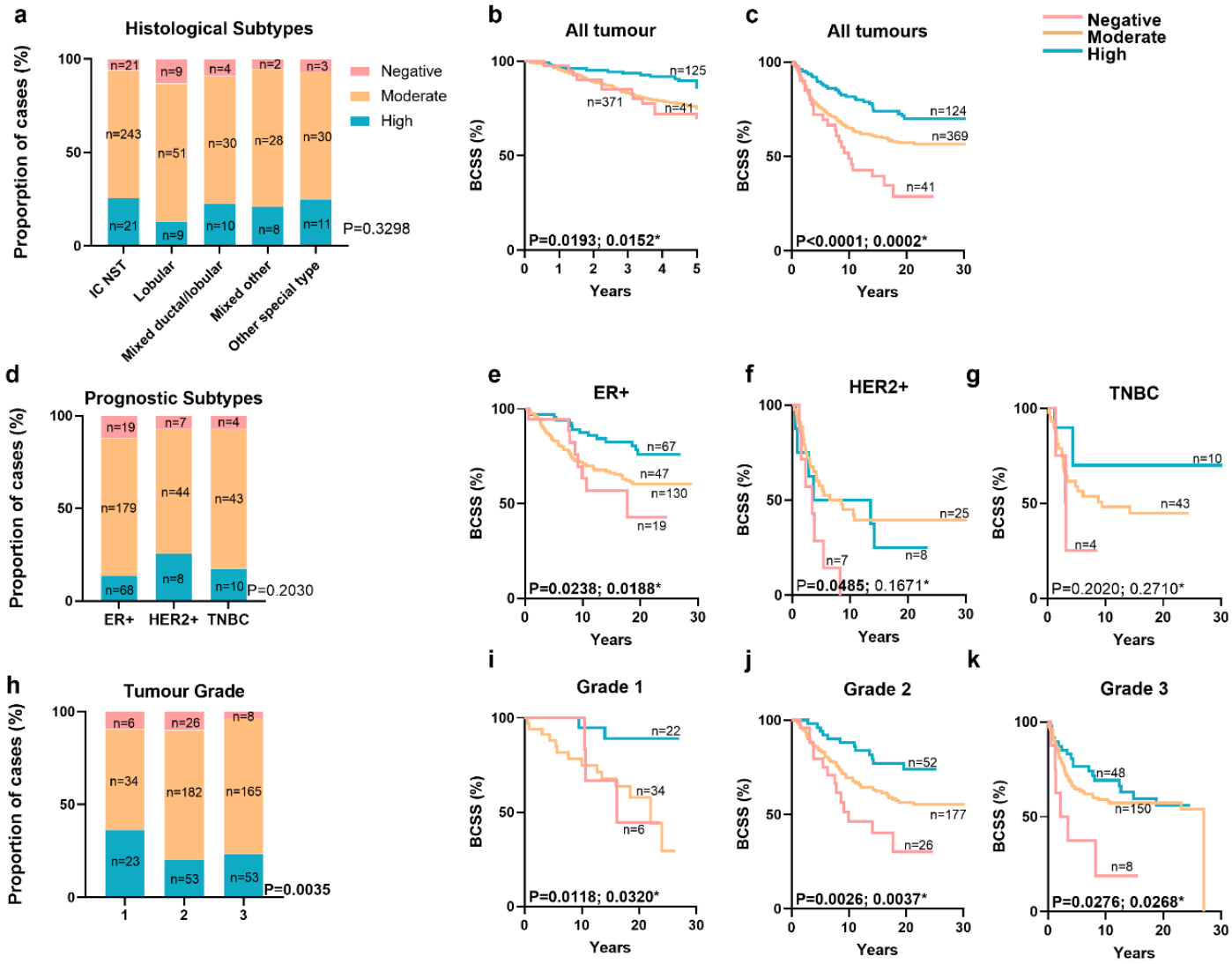


Figure 2

pSTING expression in breast tumours in the QFU cohort. (a) Chi-square analysis of the proportion of breast cancer histological subtypes with negative, moderate or high pSTING expression. **(b-c)**Kaplan–Meier (KM) analysis of pSTING expression and 5-year **(b)** and 30-year BCSS **(c)**. **(d)** Chi-square analysis of the proportion of breast cancer prognostic subtypes (ER+, HER2+, and TNBC) with negative, moderate or high pSTING expression. Kaplan–Meier (KM) analysis of pSTING expression and 30-year BCSS across **(e)** ER+, **(f)** HER2+, and **(g)**TNBC. **(h)** Chi-square analysis of the proportion of breast cancer cases with positive and negative pSTING expression compared across tumour grades. **(i-j)**Kaplan–Meier (KM) analysis of pSTING expression and 30-year BCSS across Grade 1 **(i)**, Grade 2 **(j)** and Grade 3 **(k)**. BC, breast cancer; BCSS, breast cancer specific survival; ER+, oestrogen receptor; HER2+, human epidermal growth factor receptor 2; IC-NST, invasive carcinoma of no special type; TNBC, triple negative breast cancer. Scale bar: core = 100 μm; inset 20 μm

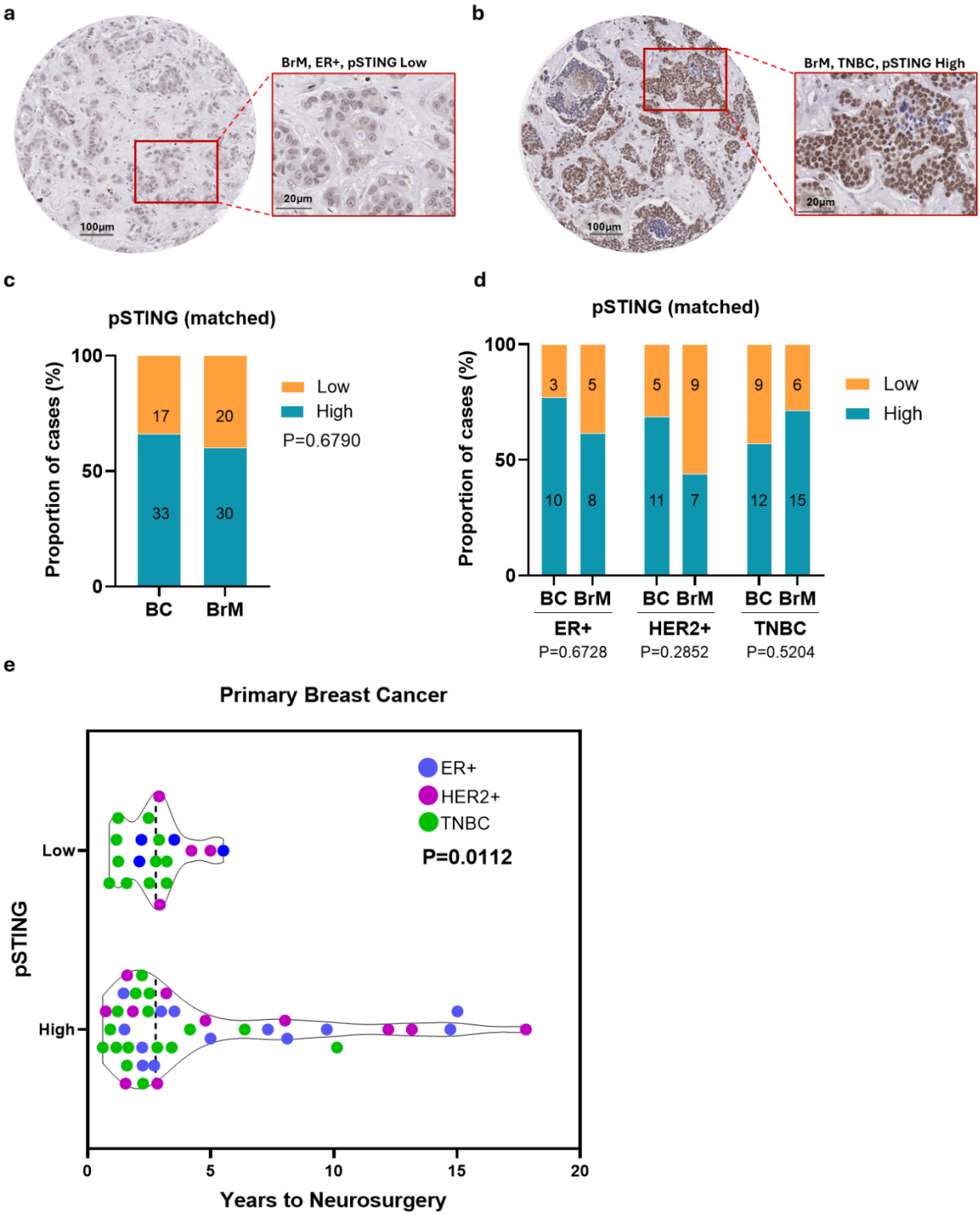


Figure 3

pSTING expression in matched breast cancer and brain metastasis tumours. Representative immunohistochemistry images of **(a)**low pSTING and **(b)** high pSTING expression in the QBBM cohort. Chi-square analysis of the proportion of matched breast cancer and brain metastasis tumours with pSTING expression **(c)** in all cases, and **(d)** compared across breast cancer prognostic subtypes. **(e)** Years taken to neurosurgery in breast cancer cases stratified by pSTING expression. BC, Breast cancer;

BrM, Brain metastasis; HER2+, human epidermal growth factor receptor 2; ER+, oestrogen receptor; TNBC, Triple negative breast cancer.

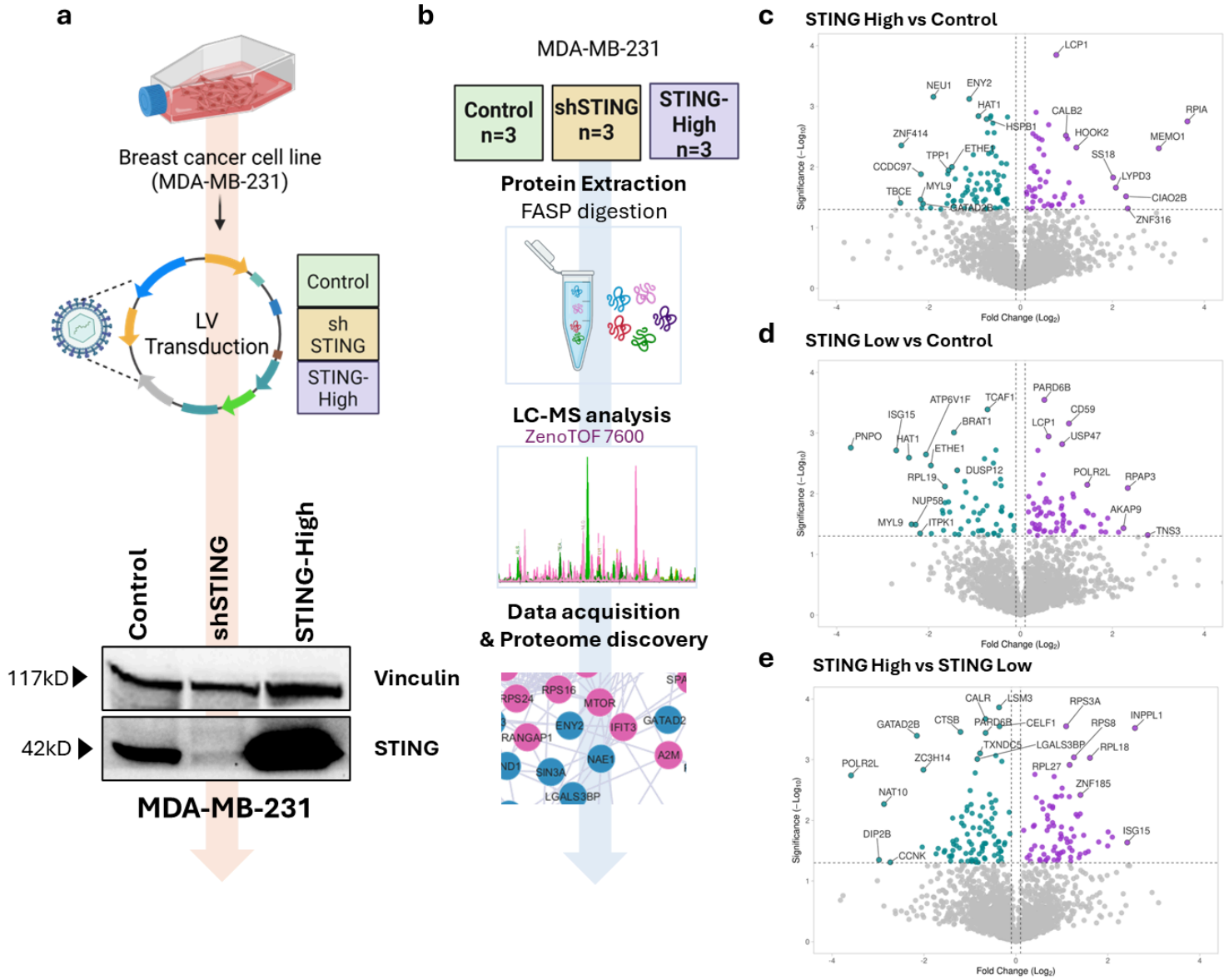


Figure 4

Workflow for Proteomics analysis. (a) Generation of STING-low and STING-high MDA-MB-231 cell lines using lentiviral vectors, with validation by western blot. **(b)** Schematic overview for protein sample preparation and LC-MS of STING modulated MDA-MB-231 cells, using filter aided sample preparation (FASP) method followed by data acquisition and analysis. Relative distribution of differentially expressed proteins (DEPs), defined by a −Log10 (p-value) ≥ 1.3 and fold change ≤ −1 or ≥ +1, in: (**c**) STING-high vs Control, (**d**) STING-low vs Control, and (e) STING-high vs STING-low cells. The top 20 significant DEPs in are labelled.

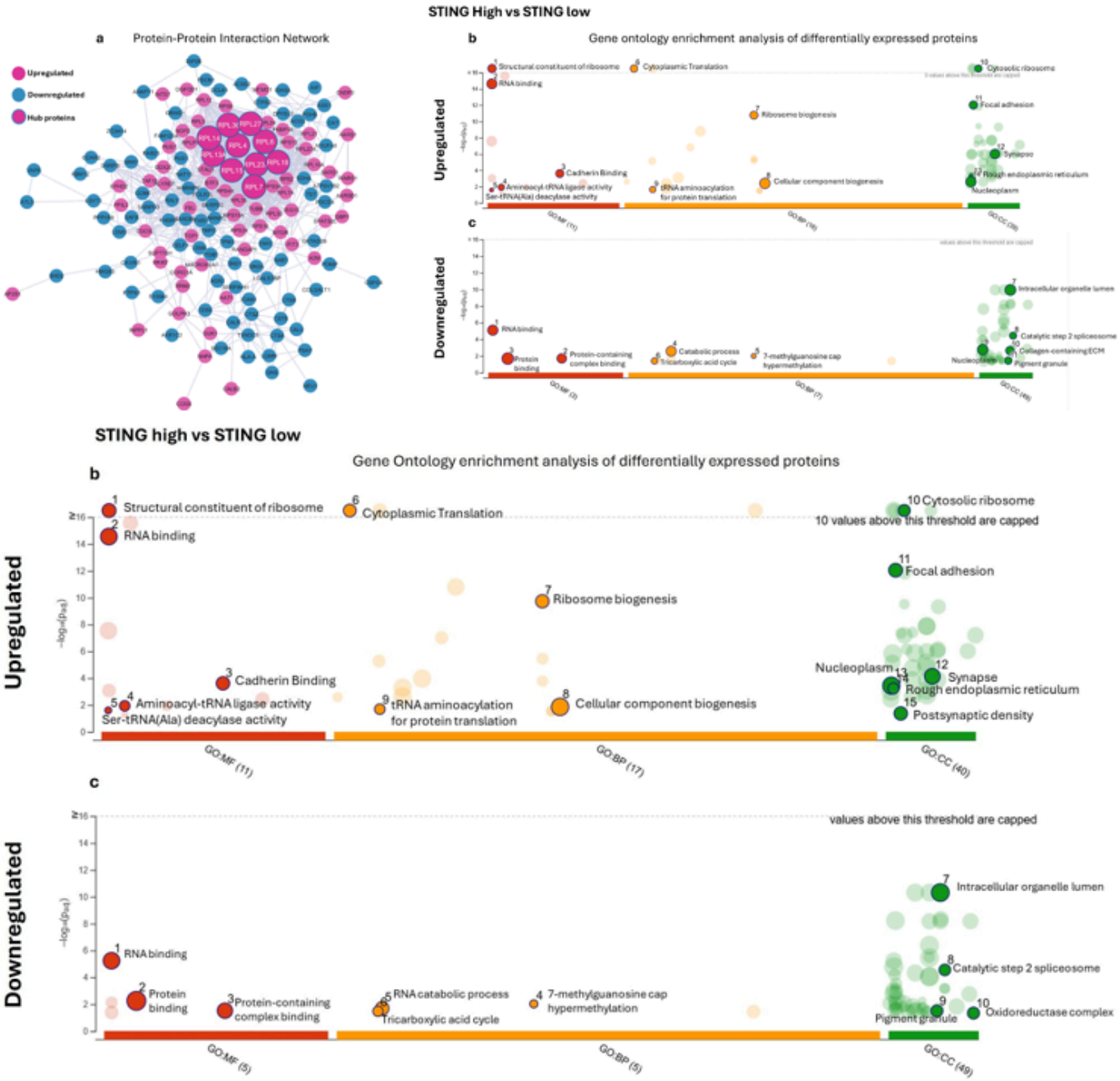


Figure 5

PPI network and Gene ontology over-representation enrichment analysis of STING-associated differentially expressed proteins in MDA-MB-231 cells. **(a)**Protein–protein interaction (PPI) network of proteins significantly upregulated (pink) or downregulated (blue) in STING-high relative to STING-low MDA-MB-231 cells. The top 10 hub proteins, identified by maximal clique centrality (MCC), are highlighted. Gene Ontology biological process enrichment analysis of **(b)** upregulated and **(c)** downregulated proteins in the STING-high versus STING-low comparison.

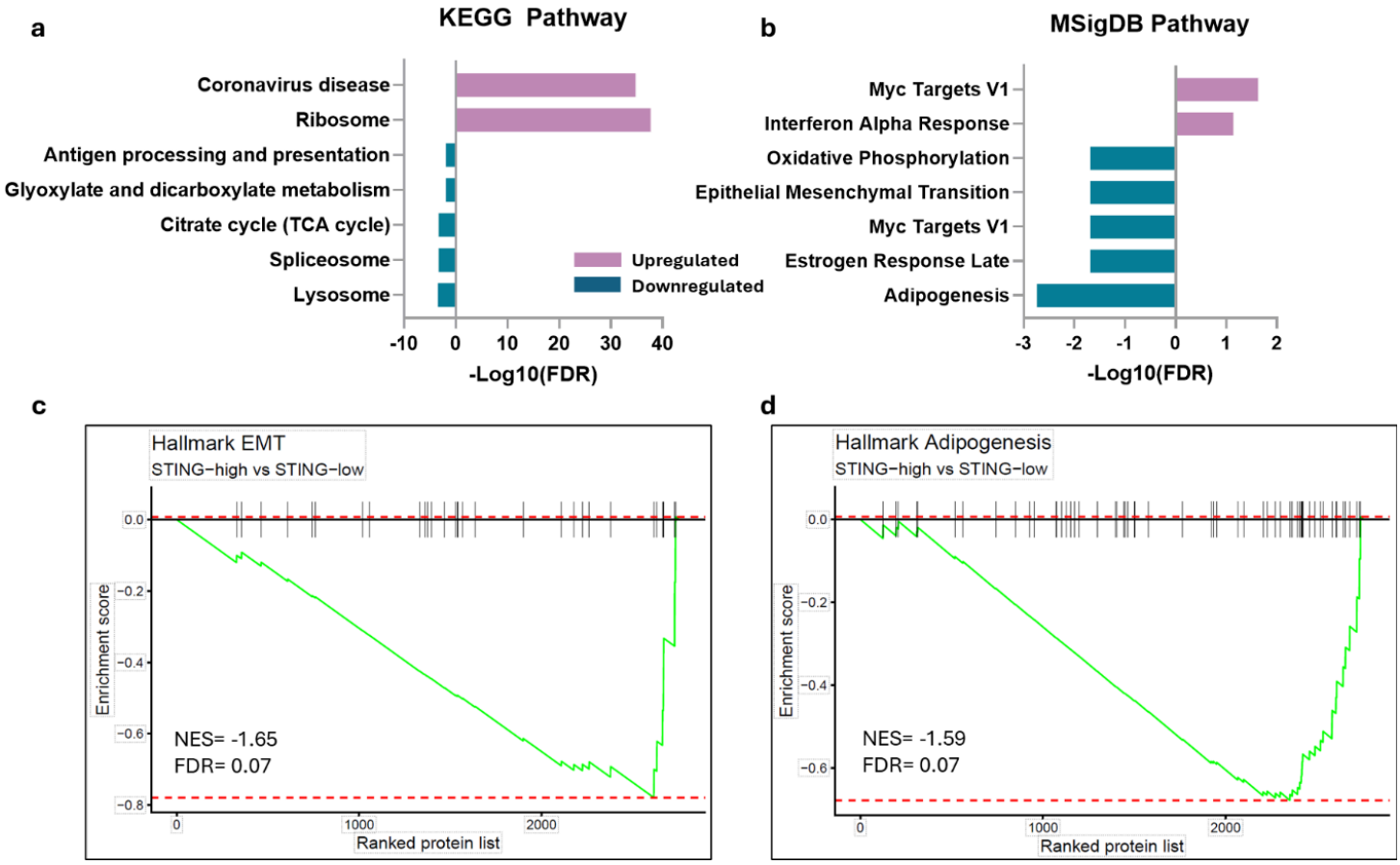


Figure 6

Over representation analysis and Gene set enrichment analysis of significant differentially expressed proteins using (a) KEGG **(b)** and MSigDB Hallmark pathway databases. Rank-based gene set enrichment analysis (GSEA) of a pre-ranked list of all quantified proteins reveals significant negative enrichment of **(c)** epithelial–mesenchymal transition and **(d)** adipogenesis pathways in STING-high relative to STING-low cells.

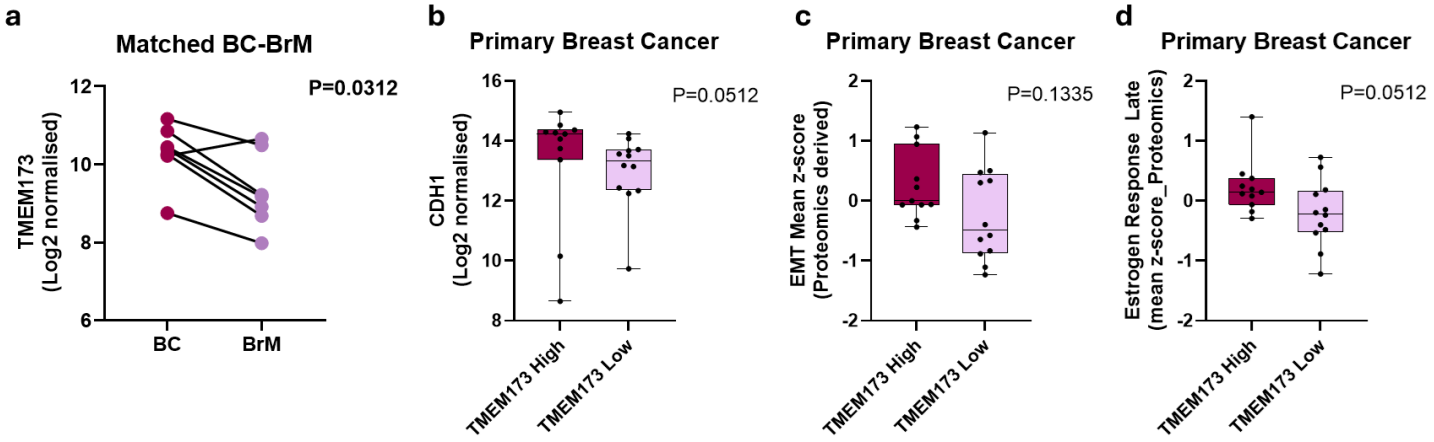


Figure 7

Gene expression analysis from AURORA breast cancer dataset (a) *TMEM173* mRNA expression in matched primary breast cancers and corresponding brain metastases from the same patients. **(b)***CDH1* mRNA expression in primary breast cancer cases stratified as STING-high or STING-low based on the median *TMEM173* expression across primary tumours **(c)** Proteomics-derived epithelial–mesenchymal transition (EMT) gene signature compared across primary breast cancer cases stratified by *TMEM173*mRNA. **(d)** Proteomics-derived Estrogen response late gene signature compared across primary breast cancer cases stratified by *TMEM173* mRNA.

Supplementary Files

This is a list of supplementary files associated with this preprint. Click to download.

- WesternblotSupplementary.docx
- JoshietalSupplementary2026.docx